RGNZ/MGPB

Rudarsko-geološko-naftni zbornik
(The Mining-Geology-Petroleum Engineering Bulletin)
DOI: 10.17794/rgn.2026.4.14

Original scientific paper

Comparative Analysis of the Performance of Palm Oil MES Surfactant and Pine Wood SLS Surfactant on Berea Sandstone in the Imbibition Process Using Neutron Computed Tomography Application

Muhammad Furqon Haryono Bimantoro[1], Rini Setiati[1]*, Fahrurrozi Akbar[2], Muhammad Taufiq Fathaddin[1], Sulistioso Giat Sukaryo[2], Bharoto Bharoto[2], Iwan Sumirat[2], Pauhesti[1], Priagung Rakhmanto[1], Refa Amelia Angelica[1]

[1] *Petroleum Engineering Department, Universitas Trisakti, Jalan Kiai Tapa, Jakarta, 11440.*

[2] *National Research and Innovation Agency (BRIN) of the Republic of Indonesia, KST B. J. Habibie, Jalan Raya Puspiptek, Muncul, Kec. Setu, Kota Tangerang Selatan, Banten, Indonesia, 15310.*

Abstract

Surfactant flooding is one of the enhanced oil recovery (EOR) methods aimed at increasing crude oil production in Indonesia. This method is implemented after primary and secondary recovery phases, by reducing the interfacial tension (IFT) in reservoir system, when a significant amount of oil remains trapped and cannot be mobilized. This study employs two types of bio-based surfactants: palm oil-derived MES (Methyl Ester Sulfonate) and pinewood-derived SLS (Sodium Lauryl Sulphate). Both are considered promising alternatives to conventional synthetic surfactants. The methodology used involves experimental and analytical laboratory research. Compatibility tests were conducted on MES and SLS solutions with concentrations ranging from 0.5% to 2% at salinities between 5,000 and 10,000 ppm, using Berea sandstone cores and light crude oil samples. The surfactants were characterized at an EOR laboratory, focusing on compatibility testing, which included aqueous stability and phase behaviour evaluations. Further analyses comprised interfacial tension measurements, IFT stability tests, and both static and dynamic adsorption assessments. Core flooding experiments were then performed on Berea cores using injection and imbibition techniques. In addition, neutron tomography imaging was utilized during core flooding to visualize surfactant distribution within the core samples, allowing identification of surfactant flow zones. Analytical calculations were conducted to validate and enhance the interpretation of the recovery factors obtained through both imbibition and injection processes.

Keywords:
middle-phase emulsion; interfacial tension; light crude oil; neutron tomography

1. Introduction

Surfactant flooding is a chemical EOR (Enhanced Oil Recovery) method designed to improve oil recovery mechanisms by mobilizing capillary-trapped residual oil following waterflooding (**Al-Jifri et al., 2021; Barati-Harooni et al., 2016**). This method depends on the effective injection and distribution of surfactant in the reservoir (**Zhao et al., 2015**). During surfactant flooding, favourable phase behaviour is targeted to achieve ultralow interfacial tension (IFT) between oil and water, allowing the trapped oil to flow easily (**Sandersen et al., 2012**). Generally, crude oil contains various surface-active components such as organic acids, salts, and alcohols. When it comes into contact with brine, natural surfactant accumulates at crude oil–brine interface, forming an adsorbed film that reduces IFT at the crude oil–water boundary (**Olajire, 2014**). The reduction in IFT minimizes the adhesive forces between oil droplets and the rock surface, thereby enabling easy mobilization toward production wells. The effectiveness of this method has been shown in previous laboratory studies (**Setiati et al., 2019, 2020, Samsol et.al, 2023**), which support proper surfactant combinations injected at low salinity levels into core samples to reduce capillarity and prevent excessive oil entrapment (**Johannessen & Spildo, 2013**).

High pressures (10–20 MPa) and temperature variations are realistic and challenging reservoir conditions in Enhanced Oil Recovery (EOR) operations. At pressures of 10–20 MPa (approximately 1,450 to 2,900 psi), which are relatively high reservoir pressures, the primary impact on surfactant flooding is dominated by temperature changes and their interaction with formation water salinity. Pressures within this range tend to maintain the fluid phase, but temperature is a critical determinant that alters surfactant chemical behaviour.

The successful application of surfactant in EOR processes depends on the ability to form microemulsions

* Corresponding author: Rini Setiati
e-mail address: rinisetiati@trisakti.ac.id

Received: 3 October 2025. Accepted: 30 March 2026.
Available online: 21 July 2026

that significantly reduce oil–water IFT in the reservoir system. In EOR systems, microemulsions are thermodynamically stable, homogeneous mixtures of immiscible fluids, namely hydrocarbons and water, stabilized by surfactant acting at the interface (**Sheng, 2011**). The system can be designed to achieve ultralow IFT values (~0.001 mN/m) by formulating stable brine or hydrocarbon phases (**Green & Willhite, 1998**), which is beneficial for EOR applications (**Alvarado & Manrique, 2010; Bealessio et al., 2021**). Furthermore, in EOR processes, a ternary diagram is focused on the three-phase region. Ternary diagram types are commonly classified as Type II (lower-phase emulsions with excess oil), Type I (+) (upper-phase emulsions with excess water), and Type III (middle-phase microemulsions) (**Du et al., 2016; Sugihardjo, 2022**). In chemical EOR, specifically surfactant flooding, microemulsions are typically categorized as Winsor Type I (lower phase), Type II (upper phase), and Type III (middle phase). Type I microemulsions are oil-in-water (O/W) in equilibrium with excess oil, Type II represents water-in-oil (W/O) in equilibrium with excess water, and Type III is a middle-phase in equilibrium with both oil and water. At optimal salinity conditions, stable middle-phase microemulsions can be formed, which significantly reduces residual oil saturation (Sor). This middle-phase also shows ultralow IFT, large interfacial surface areas, thermal stability, and the ability to solubilize both oil and water (**Sheng, 2015**). The formation of W/O or O/W emulsions in porous media is primarily influenced by contact angle, with the non-wetting phase typically becoming discontinuous, causing droplet formation (**Hu et al., 2020**). Under ultralow IFT surfactant injection, residual oil becomes highly deformable and elongated, as shown in **Figure 1**.

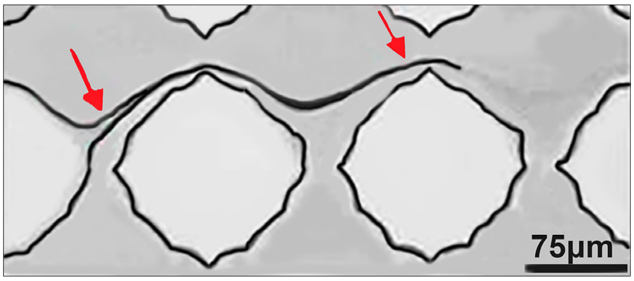

Figure 1: Residual oil condition during ultralow IFT surfactant injection (**Tagavifar et al., 2017**)

The apparent contact angle observed during immiscible displacement in porous media is governed by the balance between capillary and viscous forces, as it increases with the capillary number. In low IFT surfactant injection under water-wet reservoir conditions, the capillary number is insufficient to significantly increase the contact angle. This makes oil remain as the non-wetting phase, leading to the formation of O/W emulsions. Therefore, there is a need to understand the behaviour of contact angle by examining the underlying physics of interfacial interactions, specifically surface tension and wettability. Surface tension originates from cohesive interactions among liquid molecules. When a liquid comes into contact with another phase, whether a solid surface or a gas, an interface is formed. This interface behaves analogously to an elastic film under tension, giving rise to surface tension, and is described by two parameters, namely the contact angle (θ) and the wetting surface tension (σ, N/m). Both properties are strongly influenced by the characteristics of liquid and the nature of the adjacent phase at the interface.

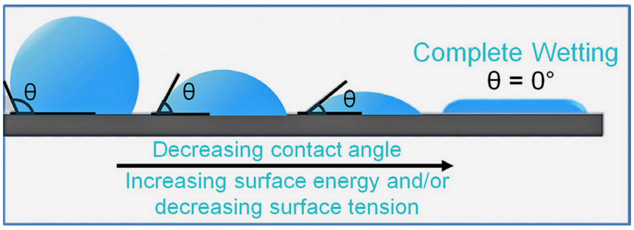

Figure 2: Variation of contact angle towards wettability (**Bolke, 2023**)

The wetting ability of surfactant is identified through the contact angle formed by liquid droplets on a solid surface. Generally, the reduction of surface or interfacial tension is also considered the most important property of surfactant in emulsion systems. In a liquid, surface molecules possess higher energy compared to those in the bulk phase. An effective surfactant, characterized by favourable contact angle and surface tension values, is expected to promote efficient wetting. A contact angle of 180° implies no interaction between the liquid and the solid substrate, indicating a non-wetting condition. When the contact angle falls between 180° and 90° (180° > θ > 90°), surfactant shows hydrophobic behaviour, favouring the stabilization of W/O emulsions with poor wettability. However, contact angles between 0° and 90° (0° < θ < 90°) signify favourable wetting, where surfactant demonstrates hydrophilic characteristics suitable for O/W emulsions, as presented in **Figure 3.**

In a water-wet reservoir with high capillary pressure, injecting low IFT surfactant can cause contact angles above 90°, promoting W/O emulsion formation rather than O/W during displacement (**Dong, 2012; J.-C. Li et al., 2020; W. Yang et al., 2021**). This is because surfactants reduce IFT between oil and water by adsorbing at their interface, displacing fluid molecules. After absorption, surfactant molecules are oriented with hydrophobic tails toward oil and hydrophilic heads toward brine. Moreover, one effective oil recovery method is spontaneous imbibition, which has been proven effective in water-wet to mixed-wet rock. This process is driven by capillary forces and gravity under low-IFT conditions. As IFT decreases, a significant transition occurs from capillary-driven spontaneous imbibition (counter-current flow) to gravity (co-current flow). Water imbibition is a physical process caused by the adsorption of water onto hydrophilic ionic groups, forming a

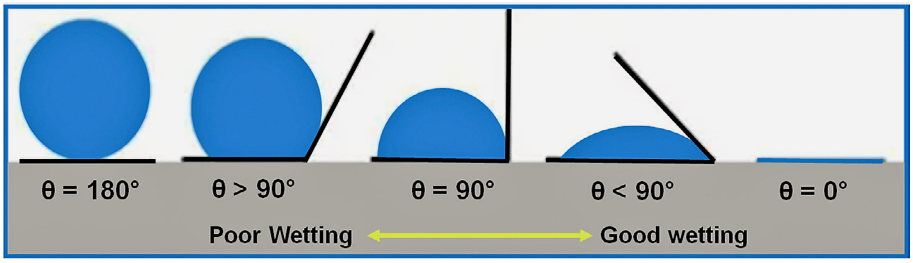

Figure 3: Wetting condition during surfactant contact angle formation (**Akbari et al., 2018**)

hydrophilic surface. In a reservoir with hydrophilic rock surfaces and lipophilic fluids such as oil, exposure to water causes spontaneous penetration to pore spaces and oil displacement. This physical phenomenon arises from forces acting within pore spaces, which are often conceptualized as capillary.

Capillary forces in porous media are influenced by mineral wettability, rock–fluid chemical interactions, and the saturation history of the reservoir. These forces play a critical role in spontaneous imbibition, a process that can be enhanced by the introduction of surfactant. The role of surfactant in imbibition is comparable to water in traditional water-driven recovery processes, reducing IFT and improving fluid displacement. The recovery factor achieved through surfactant application depends on both the rate and extent of spontaneous imbibition. In this process, displacement initially occurs through counter-current flow and gradually transitions to co-current flow. Furthermore, the capacity increases with greater contact area and higher porosity, but reduces due to higher initial water saturation (**Liu et al., 2025**).

Spontaneous imbibition is a displacement process in porous media that occurs due to differences in wettability between pore walls and fluids. This mechanism is strongly influenced by capillary pressure, which is related to wettability (**Cai et al., 2022; Dou et al., 2021; Qin, 2007; R. Yang et al., 2019**), interfacial tension (**Wang et al., 2015**), and pore radius (**Karpyn et al., 2009**). In water-wet formations, capillary forces can significantly enhance the imbibition of injected water, while in mixed-wet systems, the effect becomes negligible (**Haqparast et al., 2024**). Spontaneous imbibition experiments in porous media are among the most important methods for quantifying oil production and predicting recovery rates from reservoirs. In this procedure, oil-saturated core samples are placed into imbibition cell filled with either water or surfactant solution. The wettability of the core can be modified by pre-saturating it with crude oil. Subsequently, surfactant solution is absorbed into the core through spontaneous imbibition (**Meng et al., 2017**) and displaced oil accumulates above the water phase in Amott Cell. Numerous oil bubbles often adhere to the core surface, particularly when the crude oil has high viscosity, which can significantly reduce the accuracy of production measurements. **Mason & Morrow (2013)** reported that bubbles could be removed by gentle shaking or touching with a rod wetted with oil. Besides Amott Cell, the weighing method is also commonly used to evaluate oil production during spontaneous imbibition (**Y. Li et al., 2006**). In this method, when the core is immersed in water, the weight is recorded, and oil production is estimated based on the density difference between oil and water. However, the accuracy of this method may be compromised when oil bubbles remain attached to the core surface.

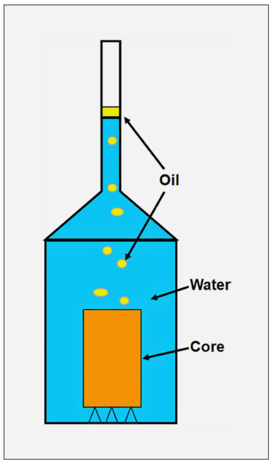

Figure 4: Amott Cell used in the spontaneous imbibition process (**Meng et al., 2017**)

Neutron tomography, is a method that generates cross-sectional images of internal structures (**Putra et al., 2015**). By rotating the sample 0°–360° under a neutron beam and capturing images at 1° intervals, detailed internal views were obtained. A CCD camera recorded each image as a 16-bit TIFF file through LabVIEW (**Bharoto et al., 2020**). These raw images were processed to analyze core samples before and after surfactant injection, showing surfactant distribution in pore spaces and enabling contact angle and volume estimation. Adsorption and wettability tests (**Civan, 2023**) complemented tomography for interpreting surfactant behaviour during fluid injection. The measurement method, which relies on neutrons generated from nuclear reactors or synchrotrons, offers distinct advantages for investigating low atomic number elements such as hydrogen and carbon (**L'Annunziata, 2016; Penumadu et al., 2016; Schwarz et al., 2005**).

Previous studies integrating porous rock samples and neutron imaging were conducted by Frikkie De Beer and F. Middleton (**de Beer et al., 2004; de Beer & Middleton, 2006; Tengattini et al., 2021**). Although the analysis did not specifically focus on reservoir rock samples, there was a significant interest in applying Neutron Computed Tomography (NCT) in the oil and gas industry (**Farrokhi et al., 2021; H. Lehmann, 2024; Hess et al., 2011; Pavan et al., 2022**). In late 2019, a collaboration between a nuclear analyst and a university in Indonesia led to an in-depth investigation of Berea sandstone samples (**Setiati et.al, 2023**). The university team developed a novel surfactant formula from sugarcane bagasse and explored both the quantitative and qualitative effects of surfactant in EOR processes (**Akbar et al., 2021**), including the visualization of Berea sandstone samples. The first phase of porosity measurement using NCT was also published (**Setiati et al., 2021**).

The assumptions and limitations of this study are partly related to the field scale. Implementing Enhanced Oil Recovery (EOR) technology from the laboratory scale to the field scale (up-scaling) is a complex process involving technical validation, mathematical modelling, and risk management. Not all successful laboratory results can be directly replicated in oil wells due to differences in volume, reservoir heterogeneity, and environmental conditions.

2. Materials and Methods

This study was conducted in a laboratory setting using core samples, which were synthetic Berea core, composed of homogeneous sandstone with specific physical properties, namely porosity and permeability, measured in the Reservoir Rock Characterization Laboratory. Each core was initially saturated using a desiccator under vacuum conditions for 24 hours, followed by brine through a core flooding apparatus to ensure that all pore spaces were filled (**Okon & Edoho, 2016**). The fluids used were synthetic formation water prepared based on a predetermined NaCl composition dissolved in D_2O, surfactant solutions at specific concentrations, made by mixing powdered surfactant (pinewood-derived SLS and palm oil-derived MES) with formation water at various salinity levels, and a light crude oil sample.

The experimental procedure consisted of several steps: preparation of synthetic formation water at salinities of 5,000 and 10,000 ppm, formulation of MES and SLS surfactant solutions at concentrations ranging from 0.5% to 1.5% and salinities between 5,000 and 10,000 ppm. The application of surfactants to injection water with salinities below 5,000 ppm (also known as Low Salinity Water-Surfactant Flooding or LSWF-S) often results in superior oil recovery efficiency compared to surfactant injection in high salinity environments (**Buktukov, 2025**). Optimal results are driven by two primary mechanisms working synergistically: More Efficient Interfacial Tension (IFT) and Wettability Alteration.

After preparation, several compatibility and performance tests were conducted with the crude oil samples. These included aqueous stability tests, phase behaviour analysis, IFT measurements, thermal stability, static and dynamic adsorption, and wettability evaluations (**Ansari, 2025, Massarweh & Abushaikha, 2020**). Based on the results of these characterizations, surfactant concentration with the most favourable properties was selected for further neutron tomography testing (**Scheffer et al., 2021**). This included imaging of dry Berea cores, brine-saturated cores, and cores subjected to the imbibition process. Core Berea has characteristics such as porosity 20-22%, permeability 400-500mD N2, length 2,4-2,6cm and diameter 2,59 cm.

After the imbibition process was completed, neutron tomography was performed on the imbibed cores **(Lohvithee et al., 2022; Luo et al., 2022**). The results were interpreted to analyze the distribution of surfactant in the core **(Mathisen et al., 1995**). Identifying the presence and distribution of surfactant enabled assessment of middle-phase emulsion formation between surfactant and oil in the system, which was associated with the reduction in IFT and improved mobilization of oil droplets from the core matrix (**Samba, 2024**).

Brine solutions were prepared to simulate reservoir conditions more accurately. The selection of brine salinity played a critical role in ensuring that the laboratory data were both accurate and representative of field conditions. Compatibility tests between surfactant and the crude oil sample were used to identify optimal performance at salinity levels of 5,000 ppm and 10,000 ppm. Brine was prepared using heavy water (D_2O) and sodium chloride (NaCl). To replicate formation water composition, 1 ppm salinity in 1000 mL of D_2O requires 1 mg of NaCl. Therefore, 5,000 ppm and 10,000 ppm brine solutions were made by dissolving 5,000 mg and 10,000 mg of NaCl, respectively, into 1 liter of D_2O. A magnetic stirrer was used to homogenize the solutions, serving as the base for preparing palm-based MES and pine-based SLS surfactant at concentrations of 0.5% and 2%. The compositions used to prepare surfactant solutions are shown in **Table 1.**

Table 1: Composition of Materials for the Preparation of Palm-Based MES Surfactant and Pine-Derived SLS Surfactant Solutions

Salinity (ppm)	Concentration (%)	Surfactant (g)	Brine (g)
5,000	0.5%	0.5	99.5
10,000	2.0%	2.0	98.0

3. Results

3.1. Spontaneous Imbibition

In the spontaneous imbibition test, Berea core samples (see **Table 2**) were saturated with light crude oil using a vacuum desiccator for 24 hours. The vacuum process ensured complete saturation by removing trapped air from the pore spaces, confirmed through the

Table 2: Core Data for Each Amott Cell

Core	Light Crude Oil (°API)	Surfactant	Salinity (ppm)
3A	39	Palm-based MES 2%	10,000
4B	39	Pine-based SLS 2%	10,000
5C	33	Palm-based MES 0.5%	5,000
6D	33	Pine-based SLS 0.5%	5,000

cessation of air bubbles. Once saturation was complete, core samples were placed into an Amott Cell filled with surfactant solution. The spontaneous imbibition process included the displacement of brine- and oil-saturated core samples by surfactant solution under static conditions at room temperature for 4 days. During this process, the wetting fluid was drawn into the pore spaces through capillary forces, displacing the resident oil. Subsequently, the expelled oil was collected and measured periodically to calculate the recovery factor, showing the effectiveness of each surfactant solution.

After 4 days of spontaneous imbibition (see **Figure 5**), the recovery factors were obtained, with Samples 3A, 4B, 5C, and 6D achieving 45.24%, 45.09%, 52.14%, and 38.68%. Among these, sample 5C, treated with 0.5% MES at a salinity of 5,000 ppm, showed the most effective oil recovery. This result showed the superior performance of MES in reducing IFT and facilitating the penetration of the wetting phase into the pore network, thereby enhancing overall recovery efficiency.

Figure 5: Spontaneous Imbibition Using Amott Cell

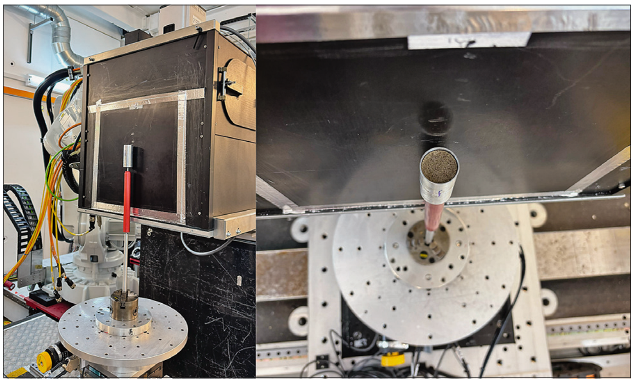

Figure 6: Core Placement in Neutron Tomography Reactor

3.2. Neuron Tomography

Neutron tomography (see **Figure 6**) was used to visualize residual oil distribution after the imbibition process. The core samples were mounted vertically, two per scan session, in a neutron imaging chamber designed to minimize external disturbances. Each scan rotated the samples 360° over approximately 12 hours to acquire high-quality tomographic images.

The 3D tomography outputs enabled the analysis of oil distribution and the identification of trapped oil zones at the microscale. This visual data provides insight into flow patterns, sweep efficiency, and the effect of surfactant formulation on displacement behaviour (**Scheffer et al., 2021**).

The contact angles formed in each system in the core ranged from 7.43° to 45.17°, indicating that the surfactant system produced relatively small contact angle (< 90°). This value was observed when the liquid spread across the surface, with values below 90° signifying favourable surface wetting. Generally, the contact angle plays a role in emulsion formation and wettability (see **Figure 8**). The results only highlight the changes observed in the study only at salinities of 5,000 and 10,000 ppm, due to the characteristics of the palm oil MES surfactant which has good performance at low salinity, not at high salinity. The application of surfactants to injection water with salinities below 5,000 ppm (also known as Low Salinity Water-Surfactant Flooding or LSWF-S) often results in superior oil recovery efficiency compared to surfactant injection in high salinity environments. Optimal results are driven by two primary mechanisms working synergistically: More Efficient Interfacial Tension (IFT) and Wettability Alteration.

Table 3: Characteristics Test Surfactant – Crude oil

Core	Light Crude Oil (°API)	Surfactant	Salinity (ppm)	IFT (mN/m)	Contact angle
3A	39	Palm-based MES 2%	10,000	1.0489	14.17
4B	39	Pine-based SLS 2%	10,000	6.9544	45.17
5C	33	Palm-based MES 0.5%	5,000	0.5130	11.79
6D	33	Pine-based SLS 0.5%	5,000	6.3147	7.43

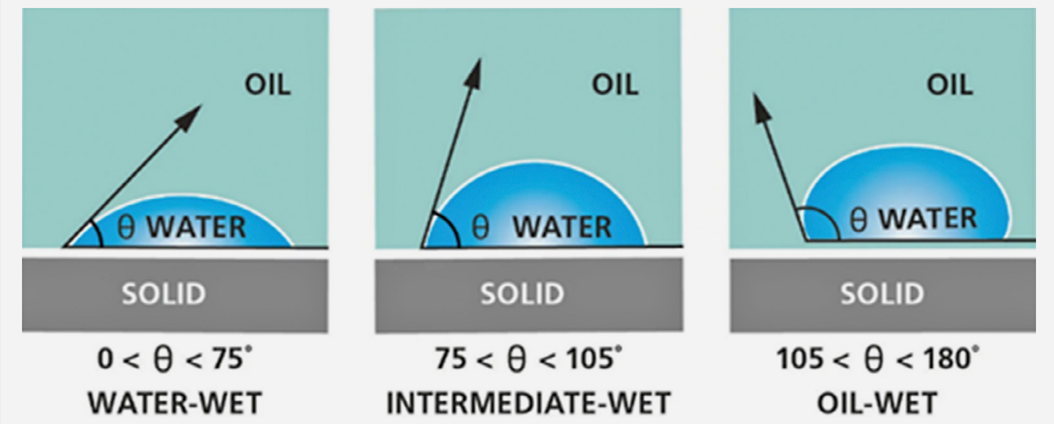

Figure 7: Contact Angle Ws Wettability (**Marmur, 2017**)

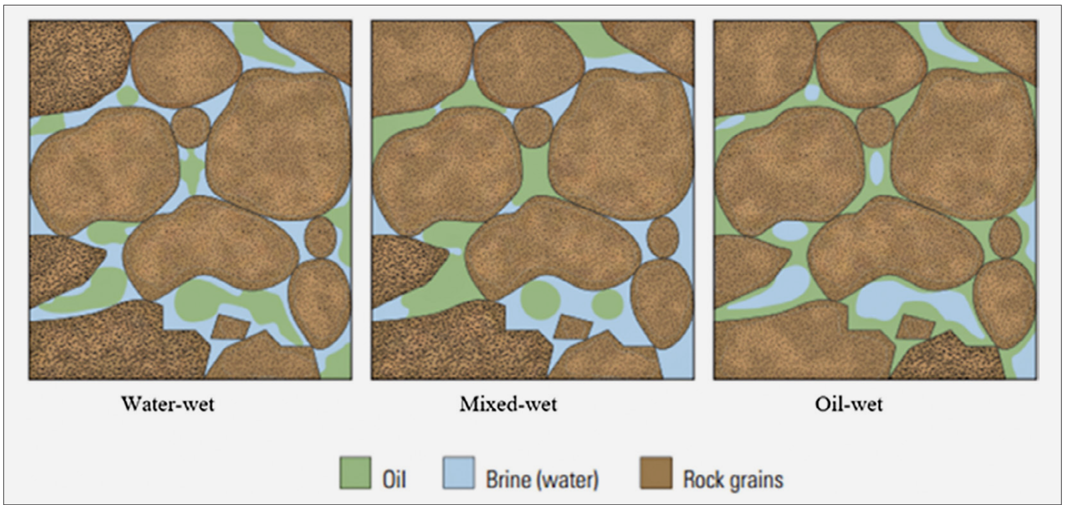

Figure 8: Type of Wettability (**Richard, 2016**)

In the context of surfactant imbibition, smaller values enhance the effectiveness of the imbibition mechanism. Based on the measured contact angle from the four core samples used in this study, all values were below 90°, confirming that the resulting wettability was water-wet. Wettability directly influences the volume of oil that can be recovered at the pore scale and is classified into water-wet and oil-wet in petroleum engineering.

In water-wet conditions, oil occupies the larger pores and becomes trapped during production due to disconnection from the main oil body. This phenomenon is observed in core samples. When a surfactant solution is introduced, there is a reduction in oil–water IFT, thereby increasing the capillary number (Nc). Furthermore, IFT serves as an indicator of solubility, with high and low values corresponding to immiscibility and miscibility in the system. At very low IFT, residual oil becomes more deformable and elongated, as shown in **Figure 7**. Evidence of miscibility can also be observed from phase changes, specifically the presence of a middle-phase emulsion. IFT formed in the surfactant–oil system influences capillary pressure, which governs fluid distribution and flow. This mechanism accounts for the measurable volume of oil obtained in an Amott Cell during spontaneous imbibition.

A total of four core samples were in this study, namely 3A, 4B, 5C, and 6D, each subjected to different treatment conditions, including variations in crude oil type, surfactant formulation, and brine salinity. Core samples 3A and 4B were saturated with crude oil of 39°API and exposed to two surfactant types prepared in brine with a salinity of 10,000 ppm. Meanwhile, 5C and 6D were saturated with crude oil of 33°API and treated with two surfactant types dissolved in brine with a salinity of 5,000 ppm. From **Table 3**, the lowest IFT value was obtained in core 5C, which was 0.5130 mN/m. With a surfactant concentration of only 0.5%, IFT could be effectively reduced.

The characteristics and concentration of surfactant influence performance in the reservoir system. Generally, the applied concentration must exceed Critical Micelle Concentration (CMC), as surfactant concentration directly impacts the reduction of IFT. Increasing concentration beyond CMC enhances the solubility of active substances due to interactions with micelle molecules, a process known as micellar solubilization. At concentra-

Table 4: Characteristics Core, Imbibition RF and Imaging NCT Test Results

Parameter	Core 3A	Core 4B	Core 5C	Core 6D
Light Crude Oil (°API)	39	39	33	33
Salinity brine (ppm)	10,000	10,000	5,000	5,000
RF Brine imbibition (%)	22.35	22.35	26.38	26.38
Type Surfactant (concentration, %)	Palm-based MES 2	Pine-based SLS 2	Palm-based MES 0.5	Pine-based SLS 0.5
IFT (mN/m)	1.0489	6.9544	0.5130	6.3147
Contact angle	14.17	45.17	11.79	7.43
Imaging NCT at surfactant imbibition	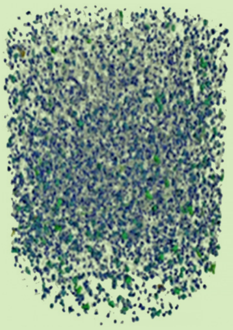	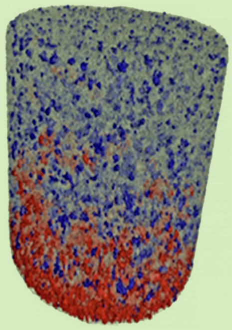	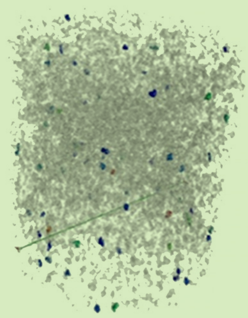	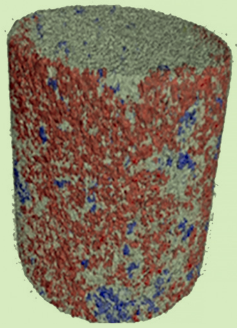
Imbibition results of oil expelled (%)	45.24	44.11	51.94	38.52

Table 5: Results of Oil Obtained Through the Imbibition Process

Core	Light Crude Oil (°API)	Surfactant	Recovery Factor (%)		Increased oil production (%)
			Water imbibition	Surfactant imbibition	
3A	39	Palm-based MES 2%	22.35	45.24	22.89
4B	39	Pine-based SLS 2%	22.35	44.11	21.76
5C	33	Palm-based MES 0.5%	26.38	51.94	25.56
6D	33	Pine-based SLS 0.5%	26.38	38.52	12.14

tions above CMC, surfactant adsorption decreases, allowing more molecules to function in lowering IFT.

In this study, neutron tomography visualization (see **Table 4**) of sample 5C showed a relatively small amount of residual oil, dispersed in isolated clusters, indicated by blue, green, and red spots unevenly distributed in the rock matrix. The application of palm-based MES surfactant at a concentration of only 0.5% with 5,000 ppm salinity successfully reduced IFT from 1.61 mN/m to 0.5130 mN/m for 33°API crude oil. Similarly, for 39°API crude oil, the same surfactant decreased IFT from 6.44 mN/m to 1.0489 mN/m. This efficiency was further shown in oil recovery factor, which reached 51.94%. When the same surfactant was applied at 2% concentration with 10,000 ppm salinity, the imbibition process achieved only 45.24% oil recovery. The higher intensity of blue spots observed in core 3A compared to core 5C showed that IFT reduction performance of palm-based MES surfactant was less effective in core 3A. These results suggested that for surfactant flooding systems, a relatively low concentration of palm-based MES surfactant (0.5%) was sufficient to achieve significant IFT reduction, without increasing the concentration to 2%. In comparison, samples 4B and 6D showed a dense and nearly uniform distribution of residual oil in the core volume. The dominance of blue and red regions in the images indicated a high remaining oil saturation. This suggested that the imbibition process using pine-based SLS was less effective in displacing oil from the pore spaces. The limited performance was attributed to the lower efficiency of pine-based SLS with the crude oil samples tested.

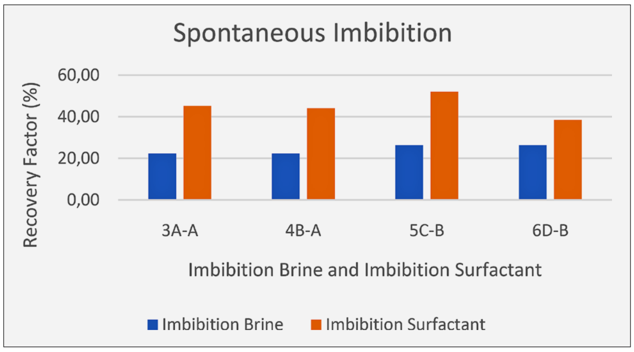

Figure 9: Result of Water Imbibition and Surfactant Imbibition

Samples 4B and 6D showed significantly different residual oil distribution patterns. In sample 4B, zonation was observed, with red-dominated regions in the lower section and bluish-grey tones in the upper section. This indicated that a significant portion of oil was retained in the lower part of the rock due to gravitational effects or limited penetration of wetting fluid. The recovery factor confirmed this observation, with 44.11% of oil successfully produced. In comparison, sample 6D showed a more extensive and uniform distribution of residual oil, characterized by a strong dominance of red coloration across the entire rock volume. This pattern showed a low imbibition efficiency, consistent with the lowest recovery factor of 38.68% (see **Figure 9**). The results suggested that pine-based SLS surfactant, when applied to the 33°API crude oil system, was only marginally effective in reducing IFT, lowering it from 1.61 mN/m to 0.513 mN/m.

The performance of palm-based MES and pine-based SLS can be evaluated through imbibition tests combined with neutron computed tomography. As shown in **Table 5** and **Figure 7**, surfactant imbibition enhances oil recovery. The best performance was observed with 0.5% palm-based MES applied to 33°API crude oil. In contrast, 39°API crude oil required a higher concentration of 2%. This difference arises from the ability of surfactant to form micelles in crude oil. For the 33°API crude sample, micellar solubilization was already achieved at 0.5%, while the same concentration was insufficient for 39°API crude. Palm-based MES showed strong performance in both 33°API and 39°API crude oil, with recovery ranging from 21.76% to 22.86%. Meanwhile, pine-based SLS showed weaker performance compared to palm-based MES. Although a 0.5% concentration of palm-based MES was sufficient, pine-based SLS required higher dosages, up to 2%, to achieve significant oil recovery. These results show that palm-based MES and pine-based SLS perform differently depending on crude oil type, enhancing the rate of recovery, but their application must be tailored to the target, light crude oil.

5. Conclusions

In conclusion, this study shows that imbibition effectiveness is strongly influenced by the type of surfactant, solution concentration, and the rock properties tested. Sample 5C shows the best performance, with the highest recovery factor of 51.94%, achieved using a palm-based MES surfactant at a concentration of 0.5% and salinity of 5,000 ppm. This is supported by tomography results, which show active imbibition zones and minimal residual oil in the upper part of the core. In comparison, sample 6D shows the lowest performance, with a recovery factor of 38.52%, where tomography visualization displays widespread and uniform residual oil distribution in the rock volume, indicating low efficiency of the imbibing fluid in mobilizing oil from the pore space. Samples 3A and 4B show approximately similar recovery factors (45.24% and 44.11%, respectively), but residual oil distribution in 3A is more localized. In 4B, residual oil distribution is denser and more dispersed, suggesting how tomography visualization can provide additional insight beyond numerical recovery values. The integration of quantitative data (recovery factor) and qualitative interpretation (tomographic images) offers a more comprehensive understanding of the imbibition behaviour in rock samples. These results show that spontaneous imbibition using palm-based MES surfactant at specific concentrations and salinities can enhance oil recovery more effectively than SLS derived from pine wood, particularly for light crude oil systems.

Surfactants are chemicals that are not cheap, but they can work effectively so they need to be assisted by reservoir simulations to bridge promising laboratory results to visible and profitable field implementation.

Acknowledgement

The authors thank the Master of Petroleum Engineering at Universitas Trisakti and National Research and Innovation Agency (BRIN) of the Republic of Indonesia, Research Centre for Radiation Detection and Nuclear Analysis Technology, for facilitating the funds and equipment for this research. Thanks also to the Directorate of Research and Community Service, Director General of Research and Development of the Ministry of Higher Education, Science and Technology for the 2025 Fiscal Year for research funding with Contract Number 124/C3/DT.05.00/PM/2025, Contract Number 1014/LL3/DT.06.01/2025 and Contract between Trisakti University and Research Grant Recipient Number 491/A/LPPM/USAKTI/VII/2025 dated June 4, 2025. The authors also extend their appreciation to the publisher for providing the opportunity for this article to be published.

6. References

Akbar, F., Ramadhani, A., Gabriel, P. K., Bharoto, & Sulistioso, G. S. (2021). Porosity measurement and petrophysical properties of the Indonesian limestone as reservoir rock by using X-ray and neutron imaging technique. *AIPC*, 020003. https://doi.org/10.1063/5.0066369

Akbari, S., Nour, A. H., Yunus, R. M., & Farhan, A. H. (2018). Biosurfactants as promising multifunctional agent: A mini review. *International Journal of Innovative Research and Scientific Studies*, *1*(1), 1–5. https://doi.org/10.53894/ijirss.v1i1.2

Al-Jifri, M., Al-Attar, H., & Boukadi, F. (2021). New proxy models for predicting oil recovery factor in waterflooded heterogeneous reservoirs. *Journal of Petroleum Exploration and Production Technology*, *11*(3), 1443–1459. https://doi.org/10.1007/s13202-021-01095-4

Ali, J. A., Kolo, K., Manshad, A. K., & Mohammadi, A. H. (2018). Recent advances in application of nanotechnology in chemical enhanced oil recovery: Effects of nanoparticles on wettability alteration, interfacial tension reduction, and flooding. *Egyptian Journal of Petroleum*, *27*(4), 1371–1383. https://doi.org/10.1016/j.ejpe.2018.09.006

Alvarado, V., & Manrique, E. (2010). Enhanced Oil Recovery: An Update Review. *Energies*, *3*(9), 1529–1575. https://doi.org/10.3390/en3091529

Ansari, M.I.; Govindarajan, S.K., Influence of low permeability barrier on hot water flooding performance – a numerical investigation, Rudarsko-geološko-naftni zbornik, Vol. 40 No. 2 (2025): No. 73, https://doi.org/10.17794/rgn.2025.2.5

Barati-Harooni, A., Najafi-Marghmaleki, A., & Mohammadi, A. H. (2016). ANFIS modeling of ionic liquids densities. *Journal of Molecular Liquids*, *224*, 965–975. https://doi.org/10.1016/j.molliq.2016.10.050

Bealessio, B. A., Blánquez Alonso, N. A., Mendes, N. J., Sande, A. V., & Hascakir, B. (2021). A review of enhanced oil recovery (EOR) methods applied in Kazakhstan. *Petroleum*, *7*(1), 1–9. https://doi.org/10.1016/j.petlm.2020.03.003

Bharoto, B., Ramadhani, A., Akbar, F., Sukaryo, S. G., Priyanto, T. H., Kurniati, M., & Fadhila, F. A. (2020). Characterization of porosity inside limestone as a reservoir of oil using neutron tomography. *Journal of Physics: Conference Series*, *1436*(1), 012007. https://doi.org/10.1088/1742-6596/1436/1/012007

Bolke, D. (2023). *Design Study for Dust Mitigation Solutions at the Tether Unit of the Nanokhod Microrover*. University of Stuttgart.

Buktukov, N., Igizbaev, R., Moldabayeva, G., Gumennikov, E. & Yesbergenova, E. (2025). ANALYSIS OF THE CAUSES OF LOW OIL RECOVERY. Rudarsko-geološko-naftni zbornik, 40 (3), 41-53. https://doi.org/10.17794/rgn.2025.3.4

Cai, J., Chen, Y., Liu, Y., Li, S., & Sun, C. (2022). Capillary imbibition and flow of wetting liquid in irregular capillaries: A 100-year review. *Advances in Colloid and Interface Science*, *304*(102654). https://doi.org/10.1016/j.cis.2022.102654

Civan, F. (2023). Petrophysical alterations – fluid disposition, distribution, and entrapment, flow functions, and petrophysical parameters of geologic formations. In *Reservoir Formation Damage* (pp. 143–179). Elsevier. https://doi.org/10.1016/B978-0-323-90228-1.00017-0

de Beer, F. C., & Middleton, M. F. (2006). Neutron radiography imaging, porosity and permeability in porous rocks. *South African Journal of Geology*, *109*(4), 541–550. https://doi.org/10.2113/gssajg.109.4.541

de Beer, F. C., Middleton, M. F., & Hilson, J. (2004). Neutron radiography of porous rocks and iron ore. *Applied Radiation and Isotopes*, *61*(4), 487–495. https://doi.org/10.1016/j.apradiso.2004.03.089

Dong, S. (2012). On imposing dynamic contact-angle boundary conditions for wall-bounded liquid–gas flows. *Computer Methods in Applied Mechanics and Engineering*, *247–248*, 179–200. https://doi.org/10.1016/j.cma.2012.07.023

Dou, L., Xiao, Y., Gao, H., Wang, R., Liu, C., & Sun, H. (2021). The study of enhanced displacement efficiency in tight sandstone from the combination of spontaneous and dynamic imbibition. *Journal of Petroleum Science and Engineering*, *199*(108327). https://doi.org/10.1016/j.petrol.2020.108327

Du, X., Lucia, L. A., & Ghiladi, R. A. (2016). A Novel Approach for Rapid Preparation of Monophasic Microemulsions That Facilitates Penetration of Woody Biomass. *ACS Sustainable Chemistry & Engineering*, *4*(3), 1665–1672. https://doi.org/10.1021/acssuschemeng.5b01601

Farrokhi, M., Jalalifar, H., & Karimi Nasab, S. (2021). An Evaluation of Cyclic Loading Conditions and Computed Tomography for the Strength and Petrophysical Properties of Anhydrite Caprock. *Rudarsko-Geološko-Naftni Zbornik*, *36*(4), 139–149. https://doi.org/10.17794/rgn.2021.4.11

Green, D. W., & Willhite, G. P. (1998). *SPE Textbook Series, Volume 6: Enhanced Oil Recovery*. Society of Petroleum Engineers.

H. Lehmann, E. (2024). Basics of Neutron Imaging. In *Nuclear Fission - From Fundamentals to Applications*. IntechOpen. https://doi.org/10.5772/intechopen.110403

Haqparast, S., Zeinabady, D., & Clarkson, C. R. (2024). Investigating the Effect of Capillary Pressure on DFIT and DFIT-FBA Analysis. *Society of Petroleum Engineers - SPE Canadian Energy Technology Conference and Exhibition, CET 2024*. https://doi.org/10.2118/218067-MS

Hess, K.-U., Flaws, A., Mühlbauer, M. J., Schillinger, B., Franz, A., Schulz, M., Calzada, E., Dingwell, D. B., & Bente, K. (2011). Advances in high-resolution neutron computed tomography: Adapted to the earth sciences. *Geosphere*, *7*(6), 1294–1302. https://doi.org/10.1130/GES00566.1

Hu, Y., Zhao, C., Zhao, J., Wang, Q., Zhao, J., Gao, D., & Fu, C. (2020). Mechanisms of fracturing fluid spontaneous imbibition behavior in shale reservoir: A review. *Journal of Natural Gas Science and Engineering*, *82*, 103498. https://doi.org/10.1016/j.jngse.2020.103498

Johannessen, A. M., & Spildo, K. (2013). Enhanced Oil Recovery (EOR) by Combining Surfactant with Low Salinity Injection. *Energy & Fuels*, *27*(10), 5738–5749. https://doi.org/10.1021/ef400596b

Karpyn, Z. T., Alajmi, A., Radaelli, F., Halleck, P. M., & Grader, A. S. (2009). X-ray CT and hydraulic evidence for a relationship between fracture conductivity and adjacent matrix porosity. *Engineering Geology*, *103*(3–4), 139–145. https://doi.org/10.1016/j.enggeo.2008.06.017

L'Annunziata, M. F. (2016). Radioactivity: Introduction and History, From the Quantum to Quarks: Second Edition. In *Radioactivity: Introduction and History, From the Quantum to Quarks: Second Edition*. https://doi.org/10.1016/C2013-0-19309-9

Li, J.-C., Lin, H., Li, K., Zhao, J.-F., & Hu, W.-R. (2020). Dynamic Behavior in a Storage Tank in Reduced Gravity Using Dynamic Contact Angle Method. *Microgravity Science and Technology*, *32*(6), 1039–1048. https://doi.org/10.1007/s12217-020-09831-x

Li, Y., Ruth, D., Mason, G., & Morrow, N. R. (2006). Pressures acting in counter-current spontaneous imbibition. *Journal of Petroleum Science and Engineering*, *52*(1–4), 87–99. https://doi.org/10.1016/j.petrol.2006.03.005

Liu, L., Wang, Y. M., Zheng, A. W., Li, J. Q., Zhang, Q., Tang, Y. W., Yang, W. X., Chen, M., & Shi, S. (2025). Experimental Investigation of Factors Influencing Spontaneous Imbibition in Shale Reservoirs. *Processes*, *13*(2), 503. https://doi.org/10.3390/pr13020503

Lohvithee, M., Rassame, S., & Hibiki, T. (2022). Applications of neutron computed tomography to thermal-hydraulics research. *Progress in Nuclear Energy*, *149*, 104262. https://doi.org/10.1016/j.pnucene.2022.104262

Luo, X., Zhang, Y., Zhou, H., He, K., Zhang, B., Zhang, D., & Xiao, W. (2022). Pore structure characterization and seepage analysis of ionic rare earth orebodies based on computed tomography images. *International Journal of Mining Science and Technology*, *32*(2), 411–421. https://doi.org/10.1016/j.ijmst.2022.02.006

Marmur, Abraham & Volpe, Claudio & Siboni, S. & Amirfazli, Alidad & Drelich, Jaroslaw. (2017). Contact angles and wettability: towards common and accurate terminology. Surface Innovations. 5. 3-8. 10.1680/jsuin.17.00002.

Mason, G., & Morrow, N. R. (2013). Developments in spontaneous imbibition and possibilities for future work. *Journal of Petroleum Science and Engineering*, *110*(268), 268–293. https://doi.org/10.1016/j.petrol.2013.08.018

Massarweh, O., & Abushaikha, A. S. (2020). The use of surfactants in enhanced oil recovery: A review of recent advances. *Energy Reports*, *6*, 3150–3178. https://doi.org/10.1016/j.egyr.2020.11.009

Mathisen, M. E., Vasiliou, A. A., Cunningham, P., Shaw, J., Justice, J. H., & Guinzy, N. J. (1995). Time-lapse crosswell seismic tomogram interpretation: Implications for heavy oil reservoir characterization, thermal recovery process monitoring, and tomographic imaging technology. *GEOPHYSICS*, *60*(3), 631–650. https://doi.org/10.1190/1.1443803

Meng, Q., Liu, H., & Wang, J. (2017). A critical review on fundamental mechanisms of spontaneous imbibition and the impact of boundary condition, fluid viscosity and wettability. *Advances in Geo-Energy Research*, *1*(1), 1–17. https://doi.org/10.26804/ager.2017.01.01

Mohammad Salehi, M., Omidvar, P., & Naeimi, F. (2017). Salinity of injection water and its impact on oil recovery absolute permeability, residual oil saturation, interfacial tension and capillary pressure. *Egyptian Journal of Petroleum*, *26*(2), 301–312. https://doi.org/10.1016/j.ejpe.2016.05.003

Okon, A., & Edoho, U. (2016). Experimental Study of Brine Concentration Effect on Reservoir Porosity and Permeability Measurement. *Journal of Scientific Research and Reports*, *12*(2), 1–9. https://doi.org/10.9734/JSRR/2016/28930

Olajire, A. A. (2014). Review of ASP EOR (alkaline surfactant polymer enhanced oil recovery) technology in the petroleum industry: Prospects and challenges. *Energy*, *77*, 963–982. https://doi.org/10.1016/j.energy.2014.09.005

Pavan, T. N. V., Devarapu, S. R., & Govindarajan, S. K. (2022). Comparative analysis on impact of water saturation on the performance of in-situ combustion. *Rudarsko-Geološko-Naftni Zbornik*, *37*(4), 167–175. https://doi.org/10.17794/rgn.2022.4.14

Penumadu, D., Kim, F., & Bunn, J. (2016). Damage of Composite Materials Subjected to Projectile Penetration Using High Resolution X-Ray Micro Computed Tomography. *Experimental Mechanics*, *56*(4), 607–616. https://doi.org/10.1007/s11340-015-0085-2

Putra, N., Sahmura Ramadhan, R., Septiadi, W. N., & Sutiarso. (2015). Visualization of the boiling phenomenon inside a heat pipe using neutron radiography. *Experimental Thermal and Fluid Science*, *66*, 13–27. https://doi.org/10.1016/j.expthermflusci.2015.02.026

Qin, B. (2007). *Numerical Study of Recovery Mechanisms in Tight Gas Reservoirs*. University of Oklahoma.

Raeisi, F., Mousavi, S. M., Hashemi, S. A., Malekpour, L., Bahrani, S., Lai, C. W., Chiang, W.-H., Babapoor, A., Mazraedoost, S., & Esmaeili, H. (2021). Application of biosurfactant as a demulsifying and emulsifying agent in the formulation of petrochemical products. In *Green Sustainable Process for Chemical and Environmental Engineering and Science* (pp. 399–422). Elsevier. https://doi.org/10.1016/B978-0-12-823380-1.00016-2

Richard Noelen Hoeksema, 2016, Wettability, Defining Series, Oilfield Review, https://www.slb.com/-/media/files/oilfield-review/defining-wettability.pdf

Samba, M. A.; Li, Y.; Liu, Z.; Amar, I. A.; Abdurrahman, M.; Anyimah, P. O., Investigating Absorption Effects on Oil Droplets in Enhanced Oil Recovery: A Force Analysis Approach, Vol. 39 No. 4 (2024): No. 70, https://doi.org/10.17794/rgn.2024.4.8

Samsol, S., Pauhesti, P., Pramadhika, H., Abidin, M.Z., Ridaliani, O., Wijayanti, P. & Nugrahanti, A. (2023). The impact of adding waste pineapple peel on the eor process to increase crude oil production. Rudarsko-geološko-naftni zbornik, 38 (5), 31-39. https://doi.org/10.17794/rgn.2023.5.3

Setiati, R., Akbar, F., Karisma, G.P., Ramadhani, A., Setiawan, S., Aditya, R., ... Sumirat, I. (2023). Application of neutron computed tomography in enhanced oil recovery for analysing oil distribution in berea sandstone using bagasse surfactant. Rudarsko-geološko-naftni zbornik, 38 (5), 87-95. https://doi.org/10.17794/rgn.2023.5.8

Sandersen, S. B., Stenby, E. H., & von Solms, N. (2012). The effect of pressure on the phase behavior of surfactant systems: An experimental study. *Colloids and Surfaces A: Physicochemical and Engineering Aspects*, *415*, 159–166. https://doi.org/10.1016/j.colsurfa.2012.09.006

Scheffer, K., Méheust, Y., Carvalho, M. S., Mauricio, M. H. P., & Paciornik, S. (2021). Enhancement of oil recovery by emulsion injection: A pore scale analysis from X-ray micro-tomography measurements. *Journal of Petroleum Science and Engineering*, *198*, 108134. https://doi.org/10.1016/j.petrol.2020.108134

Schwarz, D., Vontobel, P., Lehmann, E. H., Meyer, C. A., & Bongartz, G. (2005). Neutron tomography of internal structures of vertebrate remains: A comparison with X-ray computed tomography. *Palaeontologia Electronica*, *8*(2).

Setiati, R., Siregar, S., Marhaendrajana, T., & Wahyuningrum, D. (2019). Surfactant Flooding for EOR Using Sodium Lignosulfonate Synthesized from Bagasse. In *Enhanced Oil Recovery Processes - New Technologies*. IntechOpen. https://doi.org/10.5772/intechopen.88689

Setiati, R., Siregar, S., Marhaendrajana, T., & Wahyuningrum, D. (2020). Enhanced oil recovery using synthesized sodium lignosulfonate surfactant from bagasse as development petroleum science. *AIP Conference Proceedings*, 090015. https://doi.org/10.1063/5.0007725

Setiati, R., Sumirat, I., Sukaryo, S. G., Adisoemarta, P. S., Akbar, F., Marpaung, T., & Bharoto. (2021). Visualizations of Berea sandstone pores using neutron tomography. *IOP Conference Series: Earth and Environmental Science*, *894*(1), 012010. https://doi.org/10.1088/1755-1315/894/1/012010

Sheng, J. J. (2011). Mobility Control Requirement in EOR Processes. In *Modern Chemical Enhanced Oil Recovery* (pp. 79–100). Elsevier. https://doi.org/10.1016/B978-1-85617-745-0.00004-8

Sheng, J. J. (2015). Status of surfactant EOR technology. *Petroleum*, *1*(2), 97–105. https://doi.org/10.1016/j.petlm.2015.07.003

Shiri, Y., & Seyed Sabour, S. M. J. (2022). Analytical, experimental, and numerical study of capillary rise dynamics from inertial to viscous flow. *Physics of Fluids*, *34*(10). https://doi.org/10.1063/5.0111688

Sugihardjo, S. (2022). A Study of Spontaneous Imbibition Recovery Mechanism of Surfactant Formulated from Methyl Ester Sulfonates. *Scientific Contributions Oil and Gas*, *36*(2), 65–74. https://doi.org/10.29017/SCOG.36.2.763

Tagavifar, M., Xu, K., Jang, S. H., Balhoff, M. T., & Pope, G. A. (2017). Spontaneous and Flow-Driven Interfacial Phase Change: Dynamics of Microemulsion Formation at the Pore Scale. *Langmuir*, *33*(45), 13077–13086. https://doi.org/10.1021/acs.langmuir.7b02856

Tengattini, A., Lenoir, N., Andò, E., & Viggiani, G. (2021). Neutron imaging for geomechanics: A review. *Geomechanics for Energy and the Environment*, *27*, 100206. https://doi.org/10.1016/j.gete.2020.100206

Wang, G., Zhao, Z., Li, K., Li, A., & He, B. (2015). Spontaneous Imbibition Laws and the Optimal Formulation of Fracturing Fluid during Hydraulic Fracturing in Ordos Basin. *Procedia Engineering*, *126*, 549–553. https://doi.org/10.1016/j.proeng.2015.11.303

Yang, R., Hu, Q., He, S., Hao, F., Guo, X., Yi, J., & Sun, M. (2019). Wettability and connectivity of overmature shales in the Fuling gas field, Sichuan Basin (China). *AAPG Bulletin*, *103*(3), 653–689. https://doi.org/10.1306/09051817138

Yang, W., Fu, C., Du, Y., Xu, K., Balhoff, M. T., Weston, J., & Lu, J. (2021). Dynamic Contact Angle Reformulates Pore-Scale Fluid-Fluid Displacement at Ultralow Interfacial Tension. *SPE Journal*, *26*(03), 1278–1289. https://doi.org/10.2118/204459-PA

Zhao, L., Chen, X., Chen, L., Cao, R., Zhang, X., Liu, J., & Shan, F. (2015). Effects of oil recovery rate on water-flooding of homogeneous reservoirs of different oil viscosity. *Petroleum Exploration and Development*, *42*(3), 384–389. https://doi.org/10.1016/S1876-3804(15)30029-X

SAŽETAK

Komparativna analiza učinkovitosti MES surfaktanta palmina ulja i SLS surfaktanta borovine na pješčenjaku Berea u procesu imbibicije korištenjem neutronske kompjuterizirane tomografije

Poplavljivanje surfaktantom jedna je od metoda povećanja iscrpka nafte (engl. *Enhanced Oil Recovery*, EOR) usmjerenih na povećanje proizvodnje sirove nafte u Indoneziji. Ova metoda primjenjuje se nakon primarne i sekundarne faze proizvodnje smanjenjem međupovršinske napetosti (engl. *Interfacial tension*, IFT) u ležišnome sustavu, kada znatna količina nafte ostaje zarobljena i ne može se pokrenuti. U ovome su istraživanju korištene dvije vrste biosurfaktanata: MES (metil ester sulfonat) dobiven iz palmina ulja i SLS (natrijev lauril sulfat) dobiven iz borovine. Oba navedena surfaktanta smatraju se obećavajućim alternativama konvencionalnim sintetičkim surfaktantima. Korištena metodologija uključuje eksperimentalna i analitička laboratorijska istraživanja. Ispitivanja kompatibilnosti provedena su na MES i SLS otopinama u koncentracijama u rasponu od 0,5 % do 2 % pri salinitetu između 5 000 i 10 000 ppm uz primjenu jezgri pješčenjaka Berea i uzoraka lake sirove nafte. Ispitivanja surfaktanata provedena su u EOR laboratoriju, pri čemu je fokus stavljen na ispitivanje kompatibilnosti, što je uključivalo procjenu stabilnosti u vodi i procjenu faznoga ponašanja. Daljnje analize obuhvaćale su mjerenja međupovršinske napetosti, testove stabilnosti IFT te procjene adsorpcije u statičkim i dinamičkim uvjetima. Zatim su provedena ispitivanja poplavljivanja jezgri na jezgrama pješčenjaka Berea korištenjem tehnika injektiranja i imbibicije. Kako bi se vizualizirala distribucija surfaktanata unutar uzoraka jezgre tijekom poplavljivanja jezgre, korištena je neutronska tomografija, što je omogućilo identifikaciju zona protoka surfaktanata. Kako bi se potvrdila i unaprijedila interpretacija faktora iscrpka dobivenih procesima imbibicije i utiskivanja, provedeni su analitički izračuni.

Ključne riječi:
srednjofazna emulzija, međupovršinska napetost, lagana sirova nafta, neutronska tomografija

Author's contribution

Muhammad Furqon Haryono Bimantro (Student, Master of Petroleum Engineering) prepared cores for the imbibition process and analysis by neutron tomography, **Rini Setiati** (Dr, Petroleum Engineering, lecturer, expertise in Enhanced Oil Recovery) has proven the mechanism of action of surfactant flooding on EOR. **Fahrurrozi Akbar** (MSc, Researcher/ Instrument Scientist) performed neutron tomography data analysis, measurement and interpretation results. **Muhammad Taufiq Fathaddin** (PhD, Professor, Petroleum Engineering) analyzed the results of the neutron tomography interpretation of the performance of the oil mechanism. **Sulistioso Giat Sukaryo** (MSc, Researcher/ Material Scientist) contributed to the manuscript editing and interpretation of the results. **Bharoto Bharoto** (MSc, Researcher/ Computer Scientist) prepared the data acquisition of neutron tomography software. **Iwan Sumirat** (Dr. Eng., Researcher/ Instrument Scientist at Neutron Scattering Laboratory) set up the neutron tomography experiment method. **Pauhesti** (Petroleum Engineering, lecturer, expertise in Enhanced Oil Recovery) has proven the mechanism of action of surfactant flooding on EOR; **Priagung Rakhmanto** (PhD, Petroleum Engineering, lecturer) analysis; **Refa Amelia Angelica** (Student of Petroleum Engineering) prepared cores for the imbibition process.